



Deterministic continuous-time Virtual Reference Feedback Tuning (VRFT) with application to PID design[☆]



Simone Formentin^{a,*}, Marco C. Campi^b, Algo Carè^b, Sergio M. Savaresi^a

^a Dipartimento di Elettronica, Informazione e Bioingegneria, Politecnico di Milano, P.zza L. da Vinci 32, 20133 Milano, Italy

^b Dipartimento di Ingegneria dell'Informazione, University of Brescia, via Branze 38, 25123 Brescia, Italy

ARTICLE INFO

Article history:

Received 27 June 2018

Received in revised form 12 March 2019

Accepted 23 March 2019

Available online xxxx

Keywords:

Autotuning

PID

Virtual reference feedback tuning

ABSTRACT

In this paper, we introduce a data-driven control design method that does not rely on a model of the plant. The method is inspired by the Virtual Reference Feedback Tuning approach for data-driven controller tuning, but it is here entirely developed in a deterministic, continuous-time setting. A PID autotuner is then developed out of the proposed approach and its effectiveness is tested on an experimental brake-by-wire facility. The final performance is shown to outperform that of a benchmark model-based design method.

© 2019 Elsevier B.V. All rights reserved.

1. Introduction

In the last decades, people in systems and control have investigated data-driven controller tuning techniques aimed to design feedback controllers directly from data without the need of estimating a model of the system. In the last twenty years, a large variety of methods has been created, among which Iterative Feedback Tuning (IFT [1]), data-driven loop-shaping [2], Virtual Reference Feedback Tuning (VRFT [3–6]) and Correlation-based Tuning (CbT [7,8]). In particular, for the last two methods it has been shown in [9] that their performances compare to that of standard model-based design approaches where the model has been identified from data.

VRFT and CbT have been developed in the stochastic set-up described in [10], where the involved processes are stationary and evolve in discrete-time. The aim of the present work is to reformulate the VRFT approach into an autotuning method for industrial PID control. In this novel form, Input/Output (I/O) signals are not treated as stochastic processes and the theory can be fully interpreted in continuous time. This fact is important in practical problems, where control engineers are usually more familiar with continuous time models for many reasons (e.g., the fact that the settling time is directly related to the dominant poles of the system). We should also emphasize that the results

presented here are not obtained by simple modifications of the previous contributions [3–6]. In fact, those papers are based on tools (spectral factorization and stochastic processes) that lose their validity in the present context. To derive the results of this paper, Sobolev spaces and solutions of ODEs are instead used.

The resulting PID-VRFT algorithm lends itself to an easy implementation for the tuning of industrial PID controllers. The underlying design procedure relies on an optimization method, thoroughly developed in the paper, that establishes an equivalence between a model-reference control problem and the identification problem the PID-VRFT algorithm is based upon. This makes the method here proposed different from the majority of the existing approaches, which are either characterized by the use of semi-empirical rules or derived from model-based methods employing low-order data-driven models, [11]. This observation is very important in relation to the use of these methods because it implies that strong guarantees on the real system cannot in general be provided: on the one hand, semi-empirical rules are not based on optimization theories and one can only hope to obtain a suitable tuning for the application at hand; on the other hand, low-order models are always approximate, and modeling errors might jeopardize the performance of the closed-loop system, [12].

The effectiveness of the proposed approach is illustrated on a brake-by-wire (BBW) application. The BBW technology bears a promise of significant improvement over existing tools in the automotive industry, but it also poses new challenges for control design. Among other requirements, BBW systems demand adaptation to aging and rapid changes of the environmental conditions, like temperature, so that data-driven PID autotuning represents an interesting approach for fast control system recalibration.

[☆] The authors would like to thank F. Todeschini for his help with the experimental BBW setup.

* Corresponding author.

E-mail addresses: simone.formentin@polimi.it (S. Formentin), marco.campi@unibs.it (M.C. Campi), algo.care@unibs.it (A. Carè), sergio.savaresi@polimi.it (S.M. Savaresi).

The outline of the paper is as follows. The theoretical development of the method is presented in Section 2 (the proofs of the theorems are given in the Appendix for a better readability). In Section 3, we present the general autotuning algorithm and then concentrate more specifically on the tuning rules for the PID gains. We advise the reader interested in practical PID control that Section 3 can be read independently of the theoretical Section 2. The experimental results on the BBW facility are illustrated in Section 4. The paper ends with some final remarks in Section 5.

2. The methodology

2.1. Preliminaries on signals and systems

A complex-valued function $x(t)$ is said to be in \mathcal{L}^2 if it is measurable and square-integrable, i.e.,

$$\int_{-\infty}^{\infty} |x(\tau)|^2 d\tau < \infty.$$

According to Plancherel theorem [13], each $x(t) \in \mathcal{L}^2$ has a Fourier transform $X(\omega) \in \mathcal{L}^2$ and, vice versa, each $X(\omega) \in \mathcal{L}^2$ is the Fourier transform of a function $x(t) \in \mathcal{L}^2$. In what follows, any *signal* is a real-valued function that belongs to \mathcal{L}^2 .

Given a signal $x(t) \in \mathcal{L}^2$, if the derivative (in the weak sense of the theory of distributions, see e.g. Chapter 1 of [14]) of order i of $x(t)$, written $x^{(i)}(t)$, is in \mathcal{L}^2 for all $i \leq p$, then $x(t)$ is said to belong to \mathcal{H}^p , the Sobolev space of order p , [14].

Consider now the linear Ordinary Differential Equation (ODE) with delay τ

$$\mathcal{Z} : \sum_{i=0}^n \alpha_i v^{(i)}(t) - \sum_{i=0}^m \lambda_i x^{(i)}(t - \tau) = 0, \quad (2.1.1)$$

which links an input signal $x(t)$ to an output signal $v(t)$. An equation like \mathcal{Z} represents the dynamics of a *system*.

For notational convenience, introduce the polynomials

$$A(j\omega) = \sum_{i=0}^n (j\omega)^i \alpha_i, \quad L(j\omega) = \sum_{i=0}^m (j\omega)^i \lambda_i.$$

The ratio $Z(j\omega) = L(j\omega)e^{-j\omega\tau}/A(j\omega)$ is called the *frequency response* of \mathcal{Z} .

We assume that $\alpha_n \neq 0$ (this is not a real condition, it simply means that the largest derivative of $v(t)$ in the ODE has order n), and, for the time being, also assume that $A(j\omega) \neq 0$ for any ω (this condition is removed later). Note that this condition does not prevent the ODE to be unstable, that is, the roots of $A(s)$ can have positive real parts. If $x(t) \in \mathcal{H}^m$, then $\sum_{i=0}^m \lambda_i x^{(i)}(t - \tau)$ is in \mathcal{L}^2 , and, by Plancherel theorem, it has Fourier transform $L(j\omega)e^{-j\omega\tau}X(\omega) \in \mathcal{L}^2$. Consider $V(\omega) := [L(j\omega)e^{-j\omega\tau}/A(j\omega)]X(\omega)$. Since $|1/A(j\omega)| < C < \infty$ for all ω , $V(\omega)$ is also in \mathcal{L}^2 , so that, based again on Plancherel theorem, it is the Fourier transform of a function $v(t) \in \mathcal{L}^2$. Moreover, since $|(j\omega)^i/A(j\omega)| < C < \infty$ for all $i \leq n$, we obtain that also $(j\omega)^i V(\omega)$, which is the Fourier transform of the i th distributional derivative of $v(t)$, belongs to \mathcal{L}^2 for $i \leq n$. Thus, by Plancherel theorem, we conclude that $v(t) \in \mathcal{H}^n$.

We claim that this $v(t)$ is the *only solution* in \mathcal{L}^2 of \mathcal{Z} . To show this, note that $A(j\omega)V(\omega)$ is the Fourier transform of $\sum_{i=0}^n \alpha_i v^{(i)}(t)$. On the other hand, $A(j\omega)V(\omega) = L(j\omega)e^{-j\omega\tau}X(\omega)$, which is the Fourier transform of $\sum_{i=0}^m \lambda_i x^{(i)}(t - \tau)$. Thus,

$$\sum_{i=0}^n \alpha_i v^{(i)}(t) = \sum_{i=0}^m \lambda_i x^{(i)}(t - \tau)$$

and $v(t)$ satisfies the ODE \mathcal{Z} . It is in fact the only solution in \mathcal{L}^2 of \mathcal{Z} since any other solution is obtained by adding to this $v(t)$ a linear combination of the modes of \mathcal{Z} , i.e., the non-zero solutions of the homogeneous ODE $\sum_{i=0}^n \alpha_i v^{(i)}(t) = 0$, which are exponentials or exponentials multiplied by polynomials and are not functions of \mathcal{L}^2 .

As a short-hand notation, throughout the paper given $x(t) \in \mathcal{H}^m$ the only solution $v(t)$ of \mathcal{Z} in \mathcal{L}^2 is written as $\mathcal{Z}[x(t)]$.

The above notation $\mathcal{Z}[x(t)]$ extends to the case when $A(j\omega)$ has zeros on the imaginary axis, provided that these zeros are canceled by $X(\omega)$ so that $[L(j\omega)e^{-j\omega\tau}/A(j\omega)]X(\omega)$ is in \mathcal{L}^2 . As an example, suppose that the ODE is the integrator

$$v^{(1)}(t) - x(t) = 0,$$

and $x(t) = \text{sgn}(t)e^{-|t|}$ (which has 0 dc-component), then

$$X(\omega) = -2j\omega/(1 + \omega^2)$$

and $[L(j\omega)e^{-j\omega\tau}/A(j\omega)]X(\omega) = -2/(1 + \omega^2) \in \mathcal{L}^2$, which corresponds to $v(t) = -e^{-|t|}$.

2.2. The model-reference control problem

Let the *plant dynamics* be described by the ODE

$$\mathcal{P} : \sum_{i=0}^{n_p} a_i y^{(i)}(t) - \sum_{i=0}^{m_p} b_i u^{(i)}(t - \tau_p) = 0,$$

with input $u(t)$ and output $y(t)$. Notice that in \mathcal{P} the signals $u(t)$ and $y(t)$ play, respectively, the role of $x(t)$ and $v(t)$ in (2.1.1). The use of different symbols is advisable because in what follows we will deal with other systems, and the signals $v(t)$ and $x(t)$ will have to be substituted by the input and output signals for the specific system at hand.

We assume that $u(t)$ belongs to suitable Sobolev spaces such that $y(t)$, and all other signals that will be derived from it, are in \mathcal{L}^2 . The frequency response of \mathcal{P} is denoted as $P(j\omega)$.

The *controller dynamics* is instead described by

$$\mathcal{C}_\rho : \sum_{i=0}^{n_c} a_{c,i} u^{(i)}(t) - \sum_{i=0}^{m_c} b_{c,i} e^{(i)}(t) = 0, \quad (2.2.2)$$

whose input is $e(t) = r(t) - y(t)$, where $r(t)$ is the reference signal, the parameters $a_{c,i}$ are fixed and the parameters $b_{c,i}$ are tunable. As we shall see, the fact that the parameters $a_{c,i}$ are fixed allows us to obtain a convex formulation of the design problem (without much loss of generality, e.g., PID controllers have a fixed denominator which enforces the integral action). Notice also that the choice of m_c and n_c can be either free or constrained by the application, moreover m_c and n_c are not related to m_p and n_p (which are unknown).

As a special case, the *PID controller* is defined by

$$\mathcal{C}_\rho^{PID} : T_d u^{(2)}(t) + u^{(1)}(t) - (K_d + K_p T_d) e^{(2)}(t) - (K_p + K_i T_d) e^{(1)}(t) - K_i e(t) = 0,$$

where $\rho = [K_p, K_i, K_d]^T$ is the vector of tunable PID gains, and T_d is a fixed parameter that is normally used in PID control to prevent the control action from blowing up in case of abrupt changes of $e(t)$ (T_d introduces a “high-frequency pole” in $-\frac{1}{T_d}$ and, as a rule of thumb, it is usually chosen as twice the sampling time that is used for the computer-aided data processing). After suitable manipulations, the frequency response of \mathcal{C}_ρ^{PID} is seen to be

$$\mathcal{C}_\rho^{PID}(j\omega, \rho) = \rho^T \beta(j\omega) \quad (2.2.3)$$

where

$$\beta(j\omega) = \left[1, \frac{1}{j\omega}, \frac{j\omega}{1 + j\omega T_d} \right]^T. \quad (2.2.4)$$

In what follows, we shall often refer to controllers C_ρ (which are not necessarily PID) in their frequency response form written as

$$C(j\omega, \rho) = \rho^T \beta(j\omega) \quad (2.2.5)$$

where ρ is the tunable parameter vector and $\beta(j\omega)$ is a vector of given frequency responses.

Finally, let \mathcal{M} be an ODE of the form

$$\mathcal{M} : \sum_{i=0}^{n_M} c_i y^{(i)}(t) - \sum_{i=0}^{m_M} d_i r^{(i)}(t - \tau_M) = 0,$$

representing the desired closed-loop system (*reference model*), where the reference signal $r(t)$ is the input and $y(t)$ is the output, and let $M(j\omega)$ be its frequency response.

In the sequel, when explaining the VRFT idea, we shall have to also consider the inverse of the reference model, namely

$$\mathcal{M}^{-1} : \sum_{i=0}^{m_M} d_i r^{(i)}(t) - \sum_{i=0}^{n_M} c_i y^{(i)}(t + \tau_M) = 0,$$

which operates on $y(t)$, shifted onward by τ_M .

Moreover, let \mathcal{W}_{mr} be a system whose frequency response $W_{mr}(j\omega)$ will be used as a frequency weighting.

The problem of designing a controller in such a way that the closed-loop behavior is “as close as possible” to the behavior of the reference model \mathcal{M} is known as the *model-reference control problem*. It is formally defined as follows.

Problem 1 (*Model-reference Control Problem*). Find a controller of the form in (2.2.2) that minimizes the *model-reference cost function*

$$J_{mr}(\rho) = \int_{-\infty}^{+\infty} \left| \left(\frac{P(j\omega)C(j\omega, \rho)}{1 + P(j\omega)C(j\omega, \rho)} - M(j\omega) \right) W_{mr}(j\omega) \right|^2 d\omega. \quad (2.2.6)$$

The cost function $J_{mr}(\rho)$ in Eq. (2.2.6) penalizes the mismatch (weighted with $W_{mr}(j\omega)$) between the frequency behavior of the closed-loop control system (given by $\frac{P(j\omega)C(j\omega, \rho)}{1 + P(j\omega)C(j\omega, \rho)}$) and the frequency behavior of the reference model \mathcal{M} (given by $M(j\omega)$). Throughout, we assume that the optimal solution to **Problem 1** exists and is unique. Uniqueness of the solution is a mild requirement that prevents the controller parametrization from allowing multiple representations of the same controller. The solution to **Problem 1** is the *model-reference controller* C^o with frequency response

$$C^o(j\omega) = C(j\omega, \rho_o) = \rho_o^T \beta(j\omega),$$

where $\rho_o = \arg \min_{\rho} J_{mr}(\rho)$. Typically, ρ_o does not yield $J_{mr}(\rho_o) = 0$ (no perfect reference model matching).

If the frequency response $P(j\omega)$ of the plant is known, **Problem 1** can be directly solved to find a controller (*model-based design*). On the other hand, in many real-world applications $P(j\omega)$ is unavailable and data are used to construct an approximate solution to **Problem 1**. As we shall see in the next section, VRFT is a data-driven method that solves **Problem 1** without estimating a model of the plant (so that VRFT is a *direct approach*).

2.3. The VRFT approach

In this section, we show how the controller design in **Problem 1** can be recast into a data-driven controller identification problem that does not require estimating \mathcal{P} . We will first

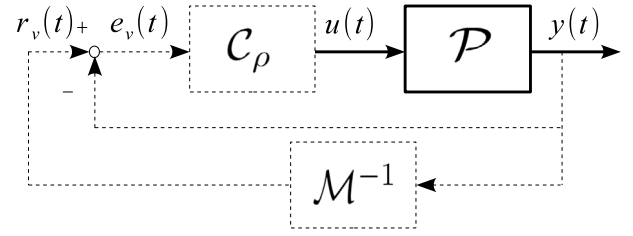


Fig. 1. Construction of signals for the VRFT algorithm. The starting point of the processing procedure is the set of measurements $u(t)$ and $y(t)$. The solid line indicates how such measurements are related to each other (namely, they are connected through the system dynamics \mathcal{P}). In dashed line, it is illustrated how the virtual reference $r_v(t)$ and the virtual error $e_v(t)$ needed by the VRFT algorithm are computed.

deal with noise-free data; noisy data will be considered in the second part of the section.

The VRFT idea. Consider the system depicted in Fig. 1. In the figure, $u(t)$ and $y(t)$ are physical signals related to each other by the plant dynamics \mathcal{P} (solid line). These signals are recorded and stored in a computer, where they are further processed off-line so as to generate other signals (“virtual signals”). The figure indicates with dashed lines the flow of information according to which the virtual signals are generated.

Precisely, the *virtual reference* signal $r_v(t)$ is computed as

$$r_v(t) = \mathcal{M}^{-1}[y(t)].$$

By making this latter expression explicit with respect to $y(t)$, one obtains $y(t) = \mathcal{M}[r_v(t)]$ and, hence, the actually measured $y(t)$ is the desired output when the reference signal is $r_v(t)$. The plant \mathcal{P} is not known, however what we know is that \mathcal{P} generates $y(t)$ when it is fed by $u(t)$. From this observation, we conclude that a “good” controller is one that generates $u(t)$ when its input is the difference between $r_v(t)$ and $y(t)$. The difference between $r_v(t)$ and $y(t)$ is called *virtual error* $e_v(t)$: $e_v(t) = r_v(t) - y(t)$.

Based on the above reasoning, the control design problem is recast as the identification problem of finding the controller that links $e_v(t)$ to $u(t)$ (*virtual-reference design*). In mathematical terms, this amounts to minimizing (with respect to ρ) the cost

$$\int_{-\infty}^{+\infty} (u(\tau) - C_\rho[e_v(\tau)])^2 d\tau. \quad (2.3.7)$$

In **Theorem 1**, we shall see that minimizing (2.3.7) gives the minimizer of $J_{mr}(\rho)$ when the controller class is large enough so that perfect reference model matching is possible. On the other hand, we will also see that one can go further by suitably filtering $u(t)$ and $e_v(t)$ before they are used in (2.3.7) and achieve an approximate solution to $J_{mr}(\rho)$ when perfect model matching is not possible (**Theorem 2**). For this reason, it is convenient to re-formulate the cost function (2.3.7) in a way that takes pre-filtering into account: letting $u_F(t)$ and $e_F(t)$ be the filtered versions of $u(t)$ and $e_v(t)$ through a filter \mathcal{F} (we shall show later criteria to choose \mathcal{F}), we define the *virtual-reference cost function* as follows

$$J_{vr}(\rho) = \int_{-\infty}^{+\infty} (u_F(\tau) - C_\rho[e_F(\tau)])^2 d\tau. \quad (2.3.8)$$

For simplicity, we assume that the minimizer of (2.3.8) exists and is unique. The uniqueness assumption is satisfied when the controller is not over-parameterized and the input signal $u(t)$ is sufficiently rich. Letting

$$\rho_{vr} = \arg \min_{\rho} J_{vr}(\rho),$$

the frequency response of the *virtual-reference controller* C_{vr} is given by

$$C(j\omega, \rho_{vr}) = \rho_{vr}^T \beta(j\omega).$$

Analysis in a noise-free setting. For analysis purposes, let us now introduce the *ideal controller* C_{id} as the controller with frequency response

$$C_{id}(j\omega) = \frac{M(j\omega)}{P(j\omega)(1 - M(j\omega))}.$$

C_{id} is the controller achieving \mathcal{M} when put in feedback interconnection with \mathcal{P} .

The first theorem that we state refers to the ideal situation where C_{id} is within the controller class and it establishes that, in this case, minimizing $J_{vr}(\rho)$ in (2.3.8) (which does not use $P(j\omega)$) is equivalent to minimizing $J_{mr}(\rho)$ in (2.2.6) (which contains $P(j\omega)$). This result holds true for any selection of the filter \mathcal{F} .

Theorem 1 (Perfect Model Matching). Assume that C_{id} belongs to the class of controllers in (2.2.2). It holds that

$$\rho_{vr} = \rho_o. \quad \square$$

Proof. See the Appendix.

Theorem 1 is fundamental in motivating the VRFT approach since, in the case where a controller with the given parametrization is sufficient to achieve the desired closed-loop behavior, it establishes the *theoretical equivalence* between model-based and data-driven design.

On the other hand, the assumption of **Theorem 1** that C_{id} is in the controller class is not realistic in many practical cases, nor can it be verified even when it is satisfied, since \mathcal{P} is unknown.

When C_{id} does not belong to (2.2.2), one still wishes to perform a suitable selection of the controller in the restricted class of controllers that is being used. **Theorem 2** shows that the optimal controller can be approximately found by suitably shaping the filter \mathcal{F} .

In preparation of **Theorem 2**, let us indicate the *mismatch* between C_{id} and C^o as the system \mathcal{D}_C with frequency response

$$D_C(j\omega) = \frac{M(j\omega)}{P(j\omega)(1 - M(j\omega))} - \rho_o^T \beta(j\omega).$$

Introduce the *extended controller* $C_{\rho^+}^+$ as a controller parameterized with $\rho^+ = [\rho^T, \delta]^T$, $\delta \in \mathbb{R}$, with frequency response

$$C^+(j\omega, \rho^+) = C(j\omega, \rho) + \delta D_C(j\omega) \quad (2.3.9)$$

and consider the *extended model-reference cost function*

$$J_{mr}^+(\rho^+) = \int_{-\infty}^{+\infty} \left| \left(\frac{P(j\omega)C^+(j\omega, \rho^+)}{1 + P(j\omega)C^+(j\omega, \rho^+)} - M(j\omega) \right) W_{mr}(j\omega) \right|^2 d\omega. \quad (2.3.10)$$

By comparing C_{id} and $C_{\rho^+}^+$, it appears that the minimizer of the extended model-reference cost function, when unique, is the extended controller $C_{\rho_o^+}^+$ with $\rho_o^+ = [\rho_o^T, 1]^T$, which gives $C_{\rho_o^+}^+ = C_{id}$ and $J_{mr}^+(\rho_o^+) = 0$.

Theorem 2 (Controller Selection When Perfect Model Matching Is Not Possible). Consider the filter frequency response

$$F(j\omega) = M(j\omega)(1 - M(j\omega))W(j\omega) \quad (2.3.11)$$

and assume that $W(j\omega)$ satisfies the condition

$$W_{mr}(j\omega) = W(j\omega)U(\omega).^1 \quad (2.3.12)$$

Then,

$$\rho_{vr} = \arg \min_{\rho} \bar{J}_{mr}^+([\rho^T, 0]^T),$$

where (recall that $\rho_o^+ = [\rho_o^T, 1]^T$)

$$\bar{J}_{mr}^+(\rho^+) = (\rho^+ - \rho_o^+)^T \frac{\partial^2 J_{mr}^+}{\partial \rho^{+2}} \Big|_{\rho_o^+} (\rho^+ - \rho_o^+) \quad (2.3.13)$$

is the second order expansion of $J_{mr}^+(\rho^+)$ around its global minimizer ρ_o^+ . \square

Proof. See the Appendix.

Theorem 2 has the following interpretation. As stated in the theorem, Eq. (2.3.13) is the second order expansion of $J_{mr}^+(\rho^+)$ around its minimizer ρ_o^+ , and **Theorem 2** asserts that ρ_{vr} minimizes this expansion over the desired class of controllers. The second order expansion well describes $J_{mr}^+(\rho^+)$ in a neighborhood of ρ_o^+ . Hence, when the class of controllers is not “too underparameterized”, i.e. the ideal controller is “close enough” to the optimal controller corresponding to $[\rho_o^T, 0]^T$, minimizing the second order expansion of $J_{mr}^+(\rho^+)$ over the given class of controllers, i.e. minimizing $\bar{J}_{mr}^+([\rho^T, 0]^T)$, returns a value close to the minimizer of $J_{mr}(\rho) = J_{mr}^+([\rho^T, 0]^T)$. Thus,

$$\rho_{vr} \approx \rho_o.$$

Dealing with noise. Consider now the case where the output $y(t)$ is corrupted by an additive noise $\eta(t) \in \mathcal{L}^2$. In this section, we shall compare the results obtained when the output is noisy with those achieved in the noise-free setting of the previous sections. Correspondingly, we are well advised to introduce the superscript ηf to indicate the noise-free components of signals, to which the results in the previous sections apply, and write, e.g.,

$$y(t) = y^{\eta f}(t) + \eta(t).$$

It can be shown that minimizing $J_{vr}(\rho)$ in (2.3.8) using noisy signals does not preserve the validity of **Theorem 1**. As an example, consider the case in which $u(t)$ and $y(t)$ are collected in open-loop (so that $u(t)$ does not depend on the noise $\eta(t)$) and note that the virtual error corresponding to the noisy output is

$$e_F(t) = e_F^{\eta f}(t) + e_F^\eta(t),$$

where $e_F^\eta(t)$ accounts for the component due to noise and has expression (superscript η indicates the component due to noise in all signals in this section)

$$e_F^\eta(t) = \mathcal{F}[\mathcal{M}^{-1}[\eta(t)] - \eta(t)].$$

Hence, the virtual reference cost function becomes

$$\begin{aligned} J_{vr}(\rho) &= \int_{-\infty}^{+\infty} (u_F(\tau) - C_\rho[e_F(\tau)])^2 d\tau \\ &= \int_{-\infty}^{+\infty} (u_F(\tau) - C_\rho[e_F^{\eta f}(\tau)])^2 d\tau \\ &\quad + \int_{-\infty}^{+\infty} (C_\rho[e_F^\eta(\tau)])^2 d\tau \\ &\quad - 2 \int_{-\infty}^{+\infty} (u_F(\tau) - C_\rho[e_F^{\eta f}(\tau)]) C_\rho[e_F^\eta(\tau)] d\tau. \end{aligned}$$

¹ The spectrum $U(\omega)$ of the signal $u(t)$ is known when $u(t)$ is selected by the control designer. More in general, the spectrum can be estimated from the input data using parametric (e.g., ARMA modeling, multiple signal classification) or nonparametric (e.g. periodogram, singular spectrum analysis) techniques as indicated in Ref. [15].

In this case, function $J_{vr}(\rho)$ is not minimized by the vector ρ_{vr} minimizing (2.3.8) in the noise-free case since the first term, which is $J_{vr}(\rho)$ in the noise-free case, is now added with two extra terms that also depend on ρ .

In this section, we show that, by building on classic *instrumental variable* methods, see e.g. [16], the VRFT procedure can be modified so as to obtain the same result ρ_{vr} as in the noise-free case even in presence of noisy data.

To start with, consider the multidimensional frequency response $\beta(j\omega)$ that appears in Eq. (2.2.5) and build the regressor

$$\varphi(t) = \beta[e_F(t)],$$

where each component of $\varphi(t)$ is obtained by filtering $e_F(t)$ by a system whose frequency response is the corresponding component of $\beta(j\omega)$. As an example, refer back to the PID case in (2.2.4). In this case, $\varphi(t)$ has three components obtained from the equations $\varphi_1(t) = e_F(t)$, $\varphi_2(t) = \int_{-\infty}^t e_F(\tau) d\tau$ and $\varphi_3^{(1)}(t) + \frac{1}{T_d}\varphi_3(t) = \frac{1}{T_d}e_F^{(1)}(t)$.

Then, consider a vector signal $\xi(t)$, called *instrumental variable*, with the same dimension of $\varphi(t)$ that satisfies the following conditions (“ > 0 ” means “positive-definite matrix”²)

$$\int_{-\infty}^{+\infty} \xi(\tau)\varphi^{nf}(\tau)^T d\tau > 0, \quad (2.3.14a)$$

$$\int_{-\infty}^{+\infty} \xi(\tau)\varphi^n(\tau)^T d\tau = 0, \quad (2.3.14b)$$

$$\int_{-\infty}^{+\infty} \xi(\tau)u_F^n(\tau)^T d\tau = 0. \quad (2.3.14c)$$

Eq. (2.3.14b) says that $\xi(t)$ is orthogonal to the component of the regressor $\varphi(t)$ due to the noise, while preserving enough correlation with the noise-free component $\varphi^{nf}(t)$ as required by (2.3.14a), and Eq. (2.3.14c) requires orthogonality between $\xi(t)$ and $u_F^n(t)$. A valid $\xi(t)$ can be obtained in various ways. At the end of this section, we will comment on a typical construction that does not make use of extra data.

Using such $\xi(t)$, build the linear equation in ρ

$$\left(\int_{-\infty}^{\infty} \xi(\tau)\varphi^T(\tau) d\tau \right) \rho = \int_{-\infty}^{\infty} \xi(\tau)u_F(\tau) d\tau. \quad (2.3.15)$$

Similarly to the noiseless case, we first consider the ideal situation where C_{id} is in the class of controllers and state [Theorem 3](#), followed by a discussion on the general case.

Theorem 3 (Noisy Data). Assume that C_{id} belongs to the class of controllers in (2.2.2) and that $\xi(t)$ satisfies (2.3.14). Then, the solution to (2.3.15) is the vector ρ_{vr} that minimizes (2.3.8) in the noise-free case. \square

Proof. See the [Appendix](#).

In the more general case where the ideal controller is not in (2.2.2), referring to the proof of [Theorem 3](#), the expression of $u_F^{nf}(t)$ in (A.7) contains a non-null term $\mathcal{D}_C[e_F^{nf}(t)]$. Referring to (A.6), the last term of this equation now becomes

$$\begin{aligned} & \Theta^{-1} \left(\int_{-\infty}^{\infty} \xi^\perp(\tau)\varphi^{nf}(\tau)^T \rho_0 d\tau + \int_{-\infty}^{\infty} \xi^\perp(\tau)\mathcal{D}_C[e_F^{nf}(\tau)] d\tau \right) \\ &= \Theta^{-1} \int_{-\infty}^{\infty} \xi^\perp(\tau)\mathcal{D}_C[e_F^{nf}(\tau)] d\tau. \end{aligned} \quad (2.3.16)$$

In general, this term is non-zero, which produces a bias in the selection of ρ . However, the bias is linear in $\mathcal{D}_C[e_F^{nf}(t)]$, which is the term that accounts for the mismatch between the ideal controller and the optimal controller, and must be small for the given class to be suitable. Moreover, $\xi(t)$ is built to mimic $\varphi^{nf}(t)$ and thus $\xi^\perp(t)$ is generally smaller than $\varphi^{nf}(t)$. Hence, the bias introduced by the extra term (2.3.16) in Eq. (A.6) is expected to be small when the VRFT method is implemented.

Referring back to the problem of constructing $\xi(t)$, when the system is operated in open-loop, one typical approach consists in feeding a model $\hat{\mathcal{P}}$ of the plant (possibly, a very coarse model built from data which is only used to generate the instrumental variable) with the input $u(t)$ to obtain a noiseless output $\hat{y}(t)$. $u(t)$ and $\hat{y}(t)$ are then used to construct $\xi(t)$ in the same way as $\varphi(t)$ is constructed from $u(t)$ and $y(t)$. Hence, $\xi(t)$ is nearly independent of $\eta(t)$ (it can bear some residual correlation with $\eta(t)$ through the construction of $\hat{\mathcal{P}}$) so that the conditions (2.3.14b) and (2.3.14c) are approximately satisfied, while it preserves enough correlation with $\varphi^{nf}(t)$ so that condition (2.3.14a) also holds true. See also the PID-VRFT algorithm of Section 3 for more details.

3. Application to PID tuning

In this section, the VRFT algorithm of the previous section is used to find handy formulas for the tuning of PID controllers. To make the resulting algorithm even easier to adopt by the end user, a simple reference model is taken and a complete VRFT-based auto-tuning architecture is provided. The effectiveness of such an approach on a real-world application is illustrated in Section 4.

To start with, let the reference model \mathcal{M} be described by the frequency response

$$M(j\omega) = \frac{e^{-j\omega\tau_M}}{(1 + j\omega 0.2t_s)^{n_M}}. \quad (3.0.17)$$

The user must assign the desired settling time t_s , the denominator degree n_M and the time delay τ_M . Notice that the time constant in $M(j\omega)$ is taken as 1/5 of the settling time t_s and $M(j0) = 1$, as it is reasonable for steady-state tracking requirements. For example, if a settling time $t_s = 1$ s is desired with $n_M = 1$ and $\tau_M = 0$, the frequency response $M(j\omega) = 1/(1 + j\omega 0.2)$ is used. When a pure delay is present in the plant \mathcal{P} and it is known to the user, such a time delay is also better included in $M(j\omega)$ by setting τ_M equal to the plant delay (if τ_M does not reflect the plant delay, stability issues may arise, see e.g. [17] for a discussion on time delays in model-reference design problems).

The user is further requested to assign a cutoff frequency f_W defining the maximum frequency at which one is interested to obtain a closed-loop system that resembles the reference model. The autotuner defined below sets

$$W(j\omega) = \frac{f_W}{j\omega + f_W}, \quad (3.0.18)$$

so that, substituting (3.0.18) in (2.3.12), gives

$$W_{mr}(j\omega) = \frac{f_W}{j\omega + f_W} U(\omega),$$

and therefore the frequency weighting of the model reference cost function is in fact given by a low pass filter with cut-off frequency f_W modulated by $U(\omega)$.

The frequency response of the PID controller is given by (2.2.3) and (2.2.4). The time constant of the derivative part T_d is selected as twice the sampling time T_s .

The interval for I/O data acquisition is denoted as $[t_0, t_f]$. In particular, if \mathcal{P} is operated in open-loop when data are acquired, the input signal $u(t)$ is injected and the corresponding output

² Recall that for a matrix A , $A > 0$ means $x^T A x > 0$, $\forall x \neq 0$ and this definition applies also when A is not symmetric.

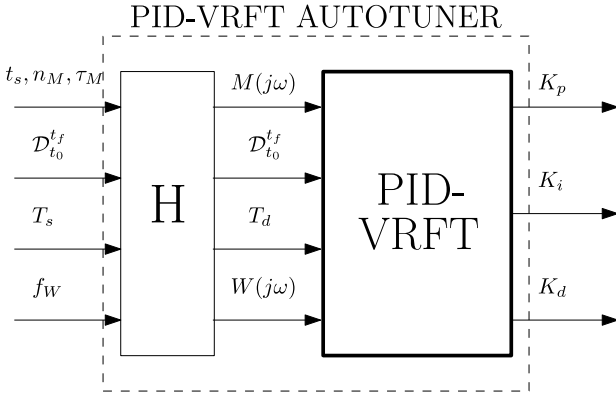


Fig. 2. The PID-VRFT autotuner layout.

signal $y(t)$ is collected. If \mathcal{P} is instead operated in closed-loop, a reference signal $r(t)$ is applied to the closed-loop system and $u(t)$ and $y(t)$ are measured. It is remarked that (differently from other existing methods) $u(t)$ or $r(t)$ are not required to be specific waveforms. In all cases, the I/O data are collected in the set

$$\mathcal{D}_{t_0}^{t_f} = \{u(t), y(t) \mid t \in [t_0, t_f]\}.$$

Notice that the theory assumes infinite-time signals (see (2.3.8)) whereas in reality $u(t)$ and $y(t)$ are known only over the finite observation window $[t_0, t_f]$. On the other hand, if the time horizon $t_f - t_0$ is long enough as compared to the time constants of the systems, then the importance of considering signals over finite time horizons is toned down and the results for the infinite horizon case hold true approximately.

Consider now the scheme depicted in Fig. 2. The overall PID-VRFT autotuner is built by linking in cascade a header block denoted by “H” with the block containing the PID-VRFT algorithm. The inputs of “H” are the above described user-chosen parameters: the settling time t_s , the denominator degree n_M and the delay τ_M of \mathcal{M} , the I/O dataset $\mathcal{D}_{t_0}^{t_f}$, the sampling time T_s and the cutoff frequency f_W of the frequency weighting. This information is used in the “H” block as indicated in the formulas (3.0.17) and (3.0.18) to construct the inputs of the PID-VRFT algorithm: $M(j\omega)$, the dataset, the derivative time constant T_d and $W(j\omega)$. The PID-VRFT block implements the VRFT algorithm for the tuning of the PID gains as described below.

PID-VRFT algorithm (inputs: $M(j\omega)$, $\mathcal{D}_{t_0}^{t_f}$, T_d , $W(j\omega)$)

1. **[Filter selection]** Consider the filter \mathcal{F} as in (2.3.11) and the auxiliary filter \mathcal{F}' with frequency response

$$F'(j\omega) = (1 - M(j\omega))W(j\omega).$$

(The filter $F'(j\omega)$ is introduced only to streamline the computation of $e_F(t)$ at point 2, where the following identity will be exploited: $e_F(t) = \mathcal{F}[\mathcal{M}^{-1}[y(t)]] - \mathcal{F}[y(t)] = \mathcal{F}'[y(t)] - \mathcal{F}[y(t)]$)

2. **[Pre-processing]** Filter $u(t)$ through \mathcal{F} to obtain $u_F(t)$ and filter $y(t)$ through \mathcal{F} and \mathcal{F}' to obtain $y_F(t)$ and $y_{F'}(t)$ respectively.

Compute $e_F(t)$ according to the formula

$$e_F(t) = y_{F'}(t) - y_F(t).$$

Build the regressor $\varphi(t)$ as

$$\varphi(t) = [\varphi_1(t) \ \varphi_2(t) \ \varphi_3(t)]^T$$

where

$$\varphi_1(t) = e_F(t),$$

$$\varphi_2(t) = \int_{t_0}^t e_F(\tau) d\tau$$

and $\varphi_3(t)$ is $e_F(t)$ filtered through a filter with frequency response

$$\Phi(j\omega) = j\omega/(1 + j\omega T_d).$$

3. **[Instrumental variable]** This step is implemented only when the plant \mathcal{P} is affected by significant noise. If not, let $\xi(t) = \varphi(t)$ and jump to step 4.

Identify a low-order model $\hat{\mathcal{P}}$ linking $u(t)$ to $y(t)$ ($\hat{\mathcal{P}}$ is only used to generate the instrumental variable and it can be a highly inaccurate model of the plant). If the data have been collected in open-loop, compute the output $\hat{y}(t)$ generated by $\hat{\mathcal{P}}$ when this system is fed with $u(t)$ (without noise). Otherwise, compute $\hat{y}(t)$ as the (noise-free) output of the closed-loop system formed by $\hat{\mathcal{P}}$ and the controller that was used in the experiment. Then, compute

$$\hat{e}_F(t) = \hat{y}_{F'}(t) - \hat{y}_F(t)$$

and define the instrumental variable $\xi(t) = \hat{\varphi}(t)$, where $\hat{\varphi}(t)$ is computed as $\varphi(t)$ in the pre-processing step by using $\hat{e}_F(t)$ instead of $e_F(t)$.

4. **[PID tuning]** Compute the PID gains according to Eqs. (3.0.19) in Box 1, where

$$x_{ij} = \int_{t_0}^{t_f} \xi_i(\tau)\varphi_j(\tau)d\tau, \quad i, j = 1, 2, 3,$$

$$x_{iu} = \int_{t_0}^{t_f} \xi_i(\tau)u_F(\tau)d\tau, \quad i = 1, 2, 3$$

and $\xi_i(t)$ and $\varphi_j(t)$ are, respectively, the i th element of $\xi(t)$ and the j th element of $\varphi(t)$. (Eqs. (3.0.19) are obtained by solving equation (2.3.15) for ρ , recalling that $\rho = [K_p, K_i, K_d]^T$.)

4. An experimental case study

The Brake-by-wire (BBW) technology aims to decouple the driver's braking command from the real actuation. Nowadays, optimal design and control of BBW actuators is one of the challenges that the automotive sector is facing. This problem has been studied in-depth for cars, while it is still an open issue for two-wheeled vehicles, since higher tracking performance is required and safety is much more critical.

Here, we consider the BBW setup for sport motorbikes depicted in Fig. 3. Such a system is composed of two parts: an electro-mechanical actuator (DC motor and transmission) and a traditional hydraulic brake, i.e. a hydraulic pump connected by means of a pipe to a caliper. The braking torque is given by the friction between the pads moved by the caliper and the disk.

In this application, the variable of interest is the braking torque. However, due to cost and reliability constraints, the torque is indirectly regulated by controlling the position y of the pump master cylinder piston by using the DC motor current as control variable u , see [18] for a more detailed description of this setup.

TUNING RULES

$$K_p = \frac{x_{12}x_{23}x_{3u} - x_{13}x_{22}x_{3u} - x_{12}x_{33}x_{2u} + x_{13}x_{32}x_{2u} + x_{22}x_{33}x_{1u} - x_{23}x_{32}x_{1u}}{x_{11}x_{22}x_{33} - x_{11}x_{23}x_{32} - x_{12}x_{21}x_{33} + x_{12}x_{23}x_{31} + x_{13}x_{21}x_{32} - x_{13}x_{22}x_{31}} \quad (3.0.19a)$$

$$K_i = \frac{-x_{11}x_{23}x_{3u} + x_{13}x_{21}x_{3u} + x_{11}x_{33}x_{2u} - x_{13}x_{31}x_{2u} - x_{21}x_{33}x_{1u} + x_{23}x_{31}x_{1u}}{x_{11}x_{22}x_{33} - x_{11}x_{23}x_{32} - x_{12}x_{21}x_{33} + x_{12}x_{23}x_{31} + x_{13}x_{21}x_{32} - x_{13}x_{22}x_{31}} \quad (3.0.19b)$$

$$K_d = \frac{x_{11}x_{22}x_{3u} - x_{12}x_{21}x_{3u} - x_{11}x_{32}x_{2u} + x_{12}x_{31}x_{2u} + x_{21}x_{32}x_{1u} - x_{22}x_{31}x_{1u}}{x_{11}x_{22}x_{33} - x_{11}x_{23}x_{32} - x_{12}x_{21}x_{33} + x_{12}x_{23}x_{31} + x_{13}x_{21}x_{32} - x_{13}x_{22}x_{31}} \quad (3.0.19c)$$

Box I.



Fig. 3. The BBW setup used in this work.

In what follows, the VRFT method proposed in this paper is applied to this control problem and its performance is compared with a model-based approach presented in the next section.

Model-based PID design. The model of the BBW setup is based on the assumption that the static Coulomb friction of the piston can be neglected. This assumption is reasonable if a dithering signal is added to the control input [19], or a friction compensator is properly designed [20,21].

Under this assumption, the following control-oriented model of the frequency response of the system linking the motor current $u(t)$ to the piston position $y(t)$ has been derived in [22]:

$$P(j\omega) = \frac{Q_{eq}}{(j\omega)^2 M_{eq} + (j\omega) R_{eq} + K_{eq}}, \quad (4.0.20)$$

where:

- M_{eq} is the equivalent mechanical inertia;
- R_{eq} is the equivalent damping (viscous friction) due to hydraulic and mechanical parts;
- K_{eq} indicates the equivalent stiffness of the overall system, including the return effect of the spring and that of the fluid pressure;
- Q_{eq} is a coefficient that, multiplied by $u(t)$, is the equivalent force applied by the motor to the master cylinder piston.

Rewrite the frequency response (4.0.20) as

$$P(j\omega) = \frac{\mu_p}{(j\omega + p_{p,1})(j\omega + p_{p,2})}. \quad (4.0.21)$$

To identify the three parameters μ_p , $p_{p,1}$ and $p_{p,2}$ of model (4.0.21), a set of I/O measurements is collected. To properly design the identification experiment, consider the following observations:

- the identification experiment is made at high piston velocity in order not to excite the nonlinear friction dynamics (according to the Stribeck model of the friction force F_f depicted in Fig. 4);
- the DC motor current is limited due to hardware constraints. Therefore, at high frequencies – where the position dynamics is strongly attenuated – it is difficult to provide the necessary power to properly excite the system;

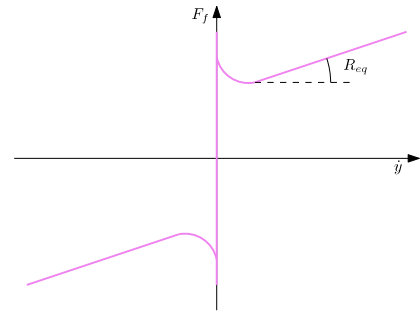


Fig. 4. The Stribeck friction model.

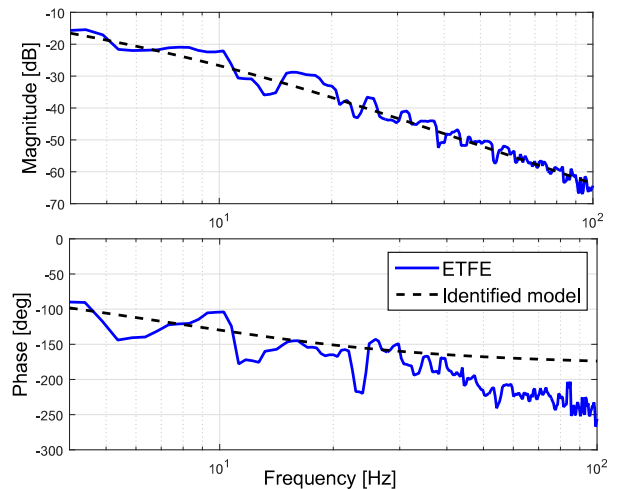


Fig. 5. ETFE and frequency response of the identified model.

- the position sensor resolution is finite, due to quantization effects, so that the input current should be large enough to make the signal-to-quantization noise ratio acceptable.

Considering the aforementioned observations, we run an experiment with a Pseudo Random Binary Sequence (PRBS) input on the physical system with 1 kHz sampling frequency and an amplitude of 8 A.

We show the results of model identification in Fig. 5, where both the Empirical Transfer Function Estimation (ETFE, solid line) and the frequency response of the identified model using Prediction Error Methods (PEM, dashed line) are shown. The identified model parameters are given in Table 1.

As for the reference model $M(j\omega)$, we consider the frequency response in (3.0.17), with $\tau_M = 0$, $n_M = 2$ and $t_s = 0.04$ s, such that the model has two poles located at $1/0.008 \approx 2\pi 20$ rad/s.

Table 1
Parameters of the identified model $P(j\omega)$ in (4.0.21).

μ_P	255.02
$p_{P,1}$	62.05
$p_{P,2}$	6.188

Table 2
PID parameters with the model-based (MB) method and the VRFT approach.

	MB	VRFT
μ_R	61.27	104.57
$z_{R,1}$	62.05	136.3
$z_{R,2}$	6.188	1.77
p_R	250	500

Now consider the PID controller of frequency response $C^{PID}(j\omega, \rho) = \rho^T \beta(j\omega)$ with $\beta(j\omega)$ as in (2.2.4) and $\rho = [K_p, K_i, K_d]^T$. It can be easily shown that such a response can be rewritten as

$$C^{PID}(j\omega, \mu_R, z_{R,1}, z_{R,2}, p_R) = \frac{\mu_R (j\omega + z_{R,1}) (j\omega + z_{R,2})}{j\omega (j\omega + p_R)}, \quad (4.0.22)$$

with straightforward definitions of p_R , μ_R , $z_{R,1}$ and $z_{R,2}$. The representation in (4.0.22) will allow us to derive more easily the model-based controller, as shown next.

Consider the model reference problem (we allow here all 4 parameters to be freely tuned, which corresponds to also see T_d as changeable)

$$\min_{\mu_R, z_{R,1}, z_{R,2}, p_R} \int_{-\infty}^{\infty} \left| \left(\frac{P(j\omega)C^{PID}(j\omega, \mu_R, z_{R,1}, z_{R,2}, p_R)}{1 + P(j\omega)C^{PID}(j\omega, \mu_R, z_{R,1}, z_{R,2}, p_R)} - M(j\omega) \right) \times W_{mr}(j\omega) \right|^2 d\omega, \quad (4.0.23)$$

where

$$W_{mr}(j\omega) = \frac{2\pi 40}{j\omega + 2\pi 40}.$$

In this particular case, by selecting the parameters to the values

$$\mu_R = \frac{1}{(0.2t_s)^2 \mu_P} \quad (4.0.24a)$$

$$z_{R,1} = p_{P,1} \quad (4.0.24b)$$

$$z_{R,2} = p_{P,2} \quad (4.0.24c)$$

$$p_R = \frac{10}{t_s}, \quad (4.0.24d)$$

the model reference cost (4.0.23) becomes exactly zero (perfect model matching solution).

Substituting the numerical values in (4.0.24) gives the PID parameters in the MB column of Table 2.

PID tuning via VRFT. The PID controller parameters are next computed by means of the PID-VRFT algorithm using the same dataset employed for system identification in the previous section; $M(j\omega)$ is as before in Eq. (4.0.23) and $W(j\omega)$ is given by (3.0.18) with $f_w = 2\pi 40$ rad/s; in the algorithm, at point 3, no instrumental variable was used, because the BBW setup is affected by low noise levels.

The resulting PID controller parameters are

$$K_p = 28.77, \quad K_i = 50.45, \quad K_d = 0.15,$$

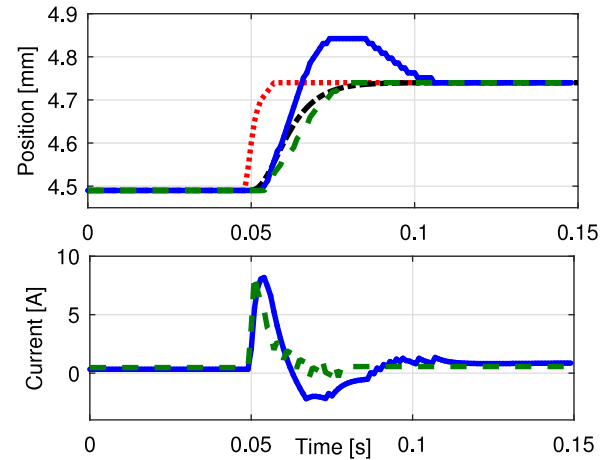


Fig. 6. Comparison between the MB and the VRFT approaches: reference signal $r(t)$ (dotted), ideal response $M[r(t)]$ (dash-dotted), output of the closed-loop with the MB controller (solid) and output of the closed-loop with the VRFT controller (dashed).

and $T_d = 2T_s = 0.002$ s, which are rewritten in the VRFT column of Table 2 in terms of μ_R , $z_{R,1}$, $z_{R,2}$, p_R for an easy comparison with the MB parameters.

Results and discussion. The MB and VRFT approaches are validated on the BBW physical setup. The reference signal (dotted line in Fig. 6) is selected as the step response of a first order low pass filter with a pole at $2\pi 60$ rad/s to avoid the saturation of the input.

Fig. 6 shows the results of the comparison, where the dash-dotted black line is the ideal response (given by $M(j\omega)$), the blue solid line is the closed-loop system output with the MB PID controller and the dashed line is the output of the closed-loop system with the VRFT PID controller. Notice that the closed-loop system with the VRFT PID controller is much closer to the ideal behavior than the one designed through the MB method. The reason is that the available data are used in VRFT towards a direct design of the controller parameters, while in the MB approach they are used to first tune a model with no concern for the final goal of controller selection, so that the imperfections in the model are bound to determine a deterioration in the closed-loop performance. In general, it is not easy to recognize which model inaccuracies are at the origin of the poor closed-loop performance with the model-based approach and, possibly, various concurrent causes determine the final effect (in Fig. 5, the difference between the ETFE and the frequency response of the identified model occurs from 40 Hz onward, beyond the closed-loop bandwidth). While it is not excluded that a more sophisticated model-based approach can get around these difficulties, it is a fact of practical interest that a method like VRFT, which *directly* uses all the information in the data to generate a controller, attains good performance with very little effort.

5. Concluding remarks

In this paper, we have developed a Virtual Reference Feedback Tuning method in a continuous time, deterministic set-up. Such a framework fits well into the classical framework of PID controller tuning. The effectiveness of the method has been demonstrated on the experimental PID tuning of a BBW actuator.

Conflict of interest

None.

Appendix

Proof of Theorem 1. In the proof, we omit to write the argument $j\omega$. Given the assumption, we can write

$$M = \frac{PC(\rho_o)}{1 + PC(\rho_o)}. \quad (\text{A.1})$$

From Plancherel Theorem, (2.3.8) can be rewritten in the frequency domain as

$$\begin{aligned} J_{vr}(\rho) &= \int_{-\infty}^{+\infty} |F|^2 |U - C(\rho)E_v|^2 d\omega \\ &= \int_{-\infty}^{+\infty} |F|^2 |1 - C(\rho)(M^{-1} - 1)P|^2 |U|^2 d\omega \\ &= \int_{-\infty}^{+\infty} \frac{|F|^2}{|M|^2} |M - C(\rho)(1 - M)P|^2 |U|^2 d\omega. \end{aligned} \quad (\text{A.2})$$

By substituting the expression (A.1) of M in (A.2), it follows that

$$\begin{aligned} \bar{J}_{vr}(\rho) &= \int_{-\infty}^{+\infty} |F|^2 \left| \frac{1 + PC(\rho_o)}{PC(\rho_o)} \right|^2 \left| \frac{P(C(\rho_o) - C(\rho))}{1 + PC(\rho_o)} \right|^2 |U|^2 d\omega \\ &= \int_{-\infty}^{+\infty} |F|^2 \frac{|C(\rho_o) - C(\rho)|^2}{|C(\rho_o)|^2} |U|^2 d\omega, \end{aligned}$$

whose minimizer ρ_{vr} is ρ_o .

Proof of Theorem 2. The first and second order derivatives of the cost $J_{mr}^+(\rho^+)$ in (2.3.10) around ρ_o^+ are, respectively,

$$\left. \frac{\partial J_{mr}^+}{\partial \rho^+} \right|_{\rho_o^+} = 0$$

$$\left. \frac{\partial^2 J_{mr}^+}{\partial \rho^{+2}} \right|_{\rho_o^+} = \int_{-\infty}^{\infty} \frac{|P|^2 |W_{mr}|^2}{|1 + PC^+(\rho_o^+)|^4} (\beta^+(\beta^{+*})^T + \beta^{+*}(\beta^+)^T) d\omega,$$

where β^+ denotes the vector $[\beta(j\omega), D_C(j\omega)]^T$, such that $\rho^{+T}\beta^+ = C^+(j\omega, \rho^+)$ (see (2.3.9)), and β^{+*} denotes its conjugate. Notice that the latter expression denotes a matrix (a 4×4 matrix in the PID case). Then, the analytical expression of $\bar{J}_{mr}^+(\rho^+)$ becomes

$$\bar{J}_{mr}^+(\rho^+) = \int_{-\infty}^{\infty} \frac{|P(C^+(\rho_o^+) - C^+(\rho^+))|^2}{|1 + PC^+(\rho_o^+)|^4} |W_{mr}|^2 d\omega.$$

By the definition of “ideal controller”, it turns out that

$$M = \frac{PC^+(\rho_o^+)}{1 + PC^+(\rho_o^+)}$$

and the above expression of $\bar{J}_{mr}^+(\rho^+)$ can be rewritten as

$$\bar{J}_{mr}^+(\rho^+) = \int_{-\infty}^{\infty} |1 - M|^2 |M - C^+(\rho^+)(1 - M)P|^2 |W_{mr}|^2 d\omega.$$

Hence, using (2.3.9),

$$\bar{J}_{mr}^+([\rho^T, 0]^T) = \int_{-\infty}^{\infty} |1 - M|^2 |M - C(\rho)(1 - M)P|^2 |W_{mr}|^2 d\omega.$$

On the other hand, the expression (A.2) for $J_{vr}(\rho)$ can be written in the light of (2.3.11) and (2.3.12) as

$$J_{vr}(\rho) = \int_{-\infty}^{\infty} |1 - M|^2 |M - C(\rho)(1 - M)P|^2 |W_{mr}|^2 d\omega.$$

Since $J_{vr}(\rho) = \bar{J}_{mr}^+([\rho^T, 0]^T)$, this concludes the proof.

Proof of Theorem 3. The vector ρ_{vr} minimizing (2.3.8) in the noise-free case satisfies the following equation

$$\left. \frac{\partial J_{vr}}{\partial \rho} \right|_{\rho_{vr}} = - \int_{-\infty}^{+\infty} \varphi^{nf}(\tau) \left(u_F^{nf}(\tau) - \varphi^{nf}(\tau)^T \rho_{vr} \right) d\tau = 0,$$

that is,

$$\left(\int_{-\infty}^{\infty} \varphi^{nf}(\tau) \varphi^{nf}(\tau)^T d\tau \right) \rho_{vr} = \int_{-\infty}^{\infty} \varphi^{nf}(\tau) u_F^{nf}(\tau) d\tau. \quad (\text{A.3})$$

On the other hand, (2.3.15) can be rewritten as

$$\begin{aligned} &\left(\int_{-\infty}^{\infty} \xi(\tau) (\varphi^{nf}(\tau)^T + \varphi^n(\tau)^T) d\tau \right) \rho \\ &= \int_{-\infty}^{\infty} \xi(\tau) (u_F^{nf}(\tau) + u_F^n(\tau)) d\tau, \end{aligned}$$

which, due to conditions (2.3.14b) and (2.3.14c), is equivalent to

$$\left(\int_{-\infty}^{\infty} \xi(\tau) \varphi^{nf}(\tau)^T d\tau \right) \rho = \int_{-\infty}^{\infty} \xi(\tau) u_F^{nf}(\tau) d\tau. \quad (\text{A.4})$$

Now, rewrite $\xi(t)$ as the sum of two components: its projection on the subspace in \mathcal{L}^2 generated by the components of the noise-free regressor $\varphi^{nf}(t)$ and a term $\xi^\perp(t)$ orthogonal to this subspace,

$$\xi(t) = \Theta \varphi^{nf}(t) + \xi^\perp(t), \quad (\text{A.5})$$

where Θ is a matrix defining the projection. Such a matrix is non-singular, as it can be seen by rewriting (2.3.14a) as

$$\begin{aligned} &\int_{-\infty}^{+\infty} (\Theta \varphi^{nf}(\tau) + \xi^\perp(\tau)) \varphi^{nf}(\tau)^T d\tau \\ &= \Theta \int_{-\infty}^{+\infty} \varphi^{nf}(\tau) \varphi^{nf}(\tau)^T d\tau \succ 0, \end{aligned}$$

and noting that the product of two matrices cannot be positive definite if one of them is singular.

Now, substitute (A.5) in (A.4) to obtain

$$\begin{aligned} &\left(\int_{-\infty}^{\infty} (\Theta \varphi^{nf}(\tau) + \xi^\perp(\tau)) \varphi^{nf}(\tau)^T d\tau \right) \rho \\ &= \int_{-\infty}^{\infty} (\Theta \varphi^{nf}(\tau) + \xi^\perp(\tau)) u_F^{nf}(\tau) d\tau, \end{aligned}$$

which reduces to

$$\begin{aligned} &\left(\int_{-\infty}^{\infty} \varphi^{nf}(\tau) \varphi^{nf}(\tau)^T d\tau \right) \rho \\ &= \int_{-\infty}^{\infty} \varphi^{nf}(\tau) u_F^{nf}(\tau) d\tau + \Theta^{-1} \int_{-\infty}^{\infty} \xi^\perp(\tau) u_F^{nf}(\tau) d\tau. \end{aligned} \quad (\text{A.6})$$

The signal $u_F^{nf}(t)$ can be seen as the output of the ideal controller C_{id} when fed by $e_F^{nf}(t)$. Therefore,

$$u_F^{nf}(t) = C_{id}[e_F^{nf}(t)] = \varphi^{nf}(t)^T \rho_o + \mathcal{D}_C[e_F^{nf}(t)]. \quad (\text{A.7})$$

Since the ideal controller is in the desired class (2.2.2), $\mathcal{D}_C[e_F^{nf}(t)] = 0$, $u_F^{nf}(t) = \varphi^{nf}(t)^T \rho_o$ and (A.6) becomes (A.3), which proves the thesis.

References

- [1] H. Hjalmarsson, M. Gevers, S. Gunnarsson, O. Lequin, Iterative feedback tuning: theory and applications, IEEE Control Syst. 18 (4) (1998) 26–41.
- [2] S. Formentin, A. Karimi, A data-driven approach to mixed-sensitivity control with application to an active suspension system, IEEE Trans. Ind. Inf. 9 (4) (2013) 2293–2300.

- [3] M. Campi, A. Lecchini, S. Savaresi, Virtual reference feedback tuning: a direct method for the design of feedback controllers, *Automatica* 38 (8) (2002) 1337–1346.
- [4] A. Lecchini, M. Campi, S. Savaresi, Virtual reference feedback tuning for two degree of freedom controllers, *Internat. J. Adapt. Control Signal Process.* 16 (5) (2002) 355–371.
- [5] M. Campi, A. Lecchini, S. Savaresi, An application of the virtual reference feedback tuning method to a benchmark problem, *Eur. J. Control* 9 (1) (2003) 66–76.
- [6] S. Formentin, A. Karimi, S. Savaresi, Optimal input design for direct data-driven tuning of model-reference controllers, *Automatica* 49 (6) (2013) 1874–1882.
- [7] K. van Heusden, A. Karimi, D. Bonvin, Data-driven model reference control with asymptotically guaranteed stability, *Internat. J. Adapt. Control Signal Process.* 25 (4) (2011) 331–351.
- [8] S. Formentin, A. Karimi, Enhancing statistical performance of data-driven controller tuning via L2-regularization, *Automatica* 50 (5) (2014) 1514–1520.
- [9] S. Formentin, K. Heusden, A. Karimi, A comparison of model-based and data-driven controller tuning, *Internat. J. Adapt. Control Signal Process.* 28 (10) (2014) 882–897.
- [10] L. Ljung, *System Identification: Theory for the User*, Prentice Hall, Upper Saddle River, NJ, 1999.
- [11] Y. Li, K. Ang, G. Chong, PID control system analysis and design, *IEEE Control Syst. Mag.* 26 (1) (2006) 32–41.
- [12] H. Hjalmarsson, From experiment design to closed-loop control, *Automatica* 41 (3) (2005) 393–438.
- [13] K. Gröchenig, *Foundations of Time-Frequency Analysis*, Springer, 2001.
- [14] R.A. Adams, J. Fournier, *Sobolev Spaces*, Academic Press, New York, 2003.
- [15] P. Stoica, R. Moses, *Spectral Analysis of Signals*, Pearson Prentice Hall, Upper Saddle River, NJ, 2005.
- [16] T. Söderström, P. Stoica, *Instrumental Variable Methods for System Identification*, in: *Lectures Notes in Control and Information Sciences*, Springer-Verlag, Berlin, 1983.
- [17] N. Nguyen, *Model-reference adaptive control: A primer*, in: *Advanced Textbooks in Control and Signal Processing*, Springer International Publishing, 2018.
- [18] F. Todeschini, G. Panzani, M. Corno, S. Savaresi, Adaptive switching position-pressure control of a brake by wire actuator for sport motorcycles, *Proc. Inst. Mech. Eng. I* (2013).
- [19] M. Michaux, A. Ferri, K. Cunefare, Effect of tangential dither signal on friction induced oscillations in an sdof model, *J. Comput. Nonlinear Dyn.* 2 (2007) 201.
- [20] G. Panzani, S. Formentin, S. Savaresi, Active motorcycle braking via direct data-driven load transfer scheduling, in: *16th IFAC Symposium on System Identification (SYSID)*, 2012, pp. 1257–1262.
- [21] R. de Castro, F. Todeschini, R.E. Araújo, S.M. Savaresi, M. Corno, D. Freitas, Adaptive-robust friction compensation in a hybrid brake-by-wire actuator, *Proc. Inst. Mech. Eng. I* (2013).
- [22] G. Panzani, M. Corno, F. Todeschini, S. Fiorenti, S. Savaresi, Analysis and control of a brake by wire actuator for sport motorcycles, in: *13th Mechatronics Forum International Conference*, Linz, Austria, September 17 2012, pp. 17–19.